Footprints of New Physics in $b \to c\tau\nu$ Transitions

Zhuoran Huang

Institute of High Energy Physics, CAS
huangzr@ihep.ac.cn

In collaboration with Ying Li, Cai-Dian Lü, Ali Paracha and Chao Wang

January 24, 2019

The LHC Landscape

Years have passed since the LHC first collisions. Experimental data is almost SM-like except that the LHCb Collaboration still holds out against the SM...

B amomalies:
b$\to$s: $R(K^{(*)})$, P_5' ...
b$\to$c: $R(D^{(*)})$,
$R(J/\psi)$

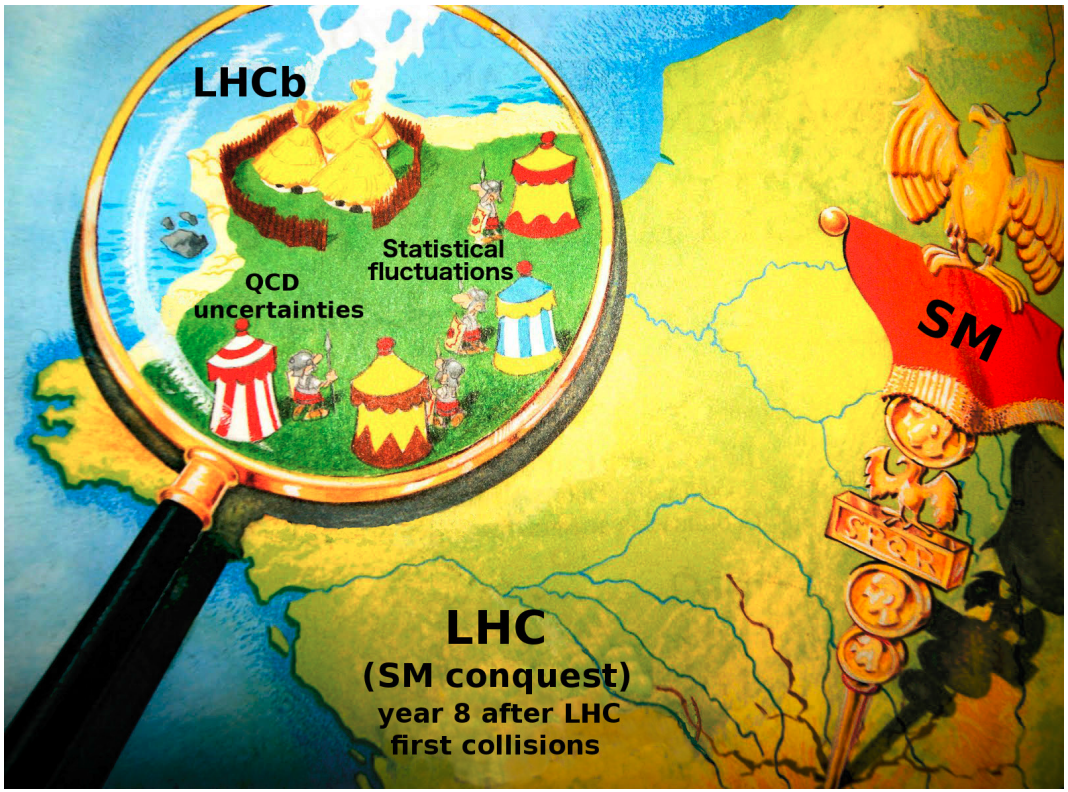

Experimental Status

- The combined results of $R(D^{(*)}) = \frac{\mathcal{B}(B \to D^{(*)}\tau\nu)}{\mathcal{B}(B \to D^{(*)}\ell\nu)}$ indicate 2.3σ and 3.4σ deviations form the SM predictions.

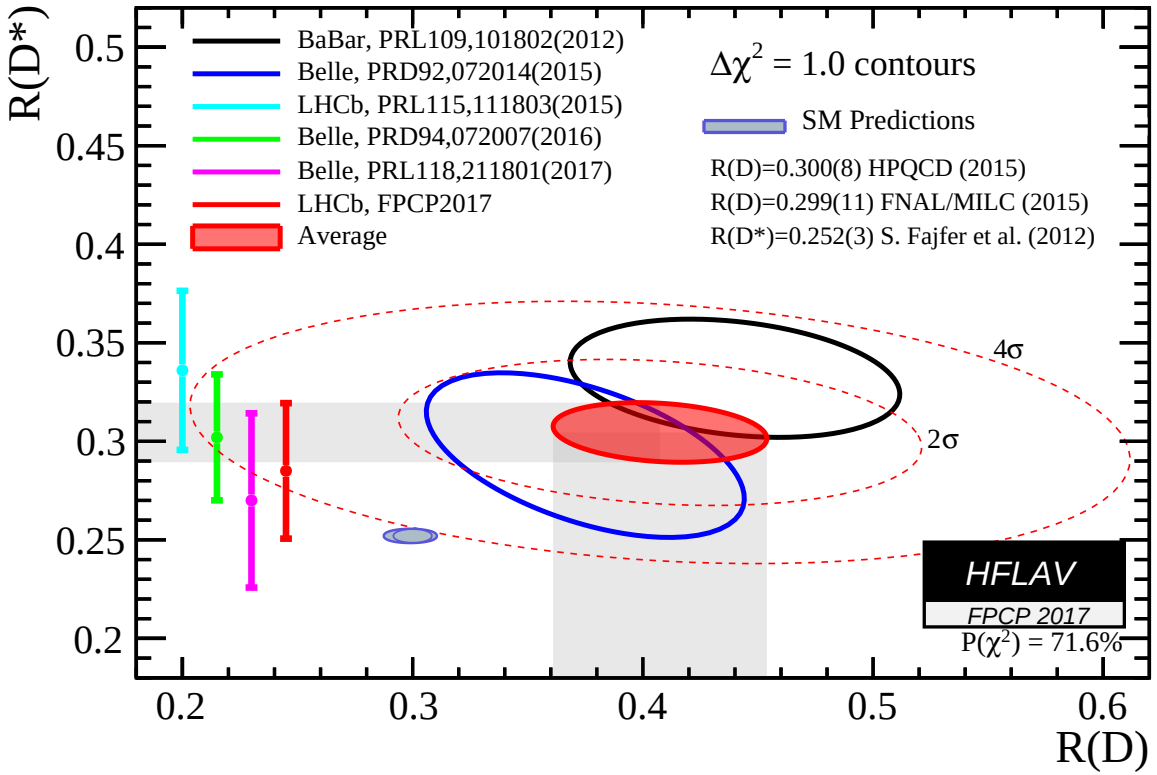

- LHCb reported $R(J/\psi) = \frac{\mathcal{B}(B_c \to J/\psi\tau\nu)}{\mathcal{B}(B_c \to J/\psi\mu\nu)} = 0.71 \pm 0.17 \pm 0.18$ that deviate 2σ away from the SM predictions.

Effective Hamiltonian

- The basic starting point for doing phenomenology in weak decays of hadrons is the weak effective Hamiltonian

$$H_{eff} = \frac{G_F}{\sqrt{2}} \sum_i V_{CKM}^i C_i(\mu) O_i$$

- For the $b \to c\tau\nu$ transition, the four-fermion operator basis can be defined as

$$\mathcal{O}_{S_1} = (\overline{c}_L b_R)(\overline{\tau}_R \nu_L)\,, \quad \mathcal{O}_{S_2} = (\overline{c}_R b_L)(\overline{\tau}_R \nu_L)\,,$$
$$\mathcal{O}_{V_1} = (\overline{c}_L \gamma^\mu b_L)(\overline{\tau}_L \gamma_\mu \nu_L)\,, \quad \mathcal{O}_{V_2} = (\overline{c}_R \gamma^\mu b_R)(\overline{\tau}_L \gamma_\mu \nu_L)\,,$$
$$\mathcal{O}_T = (\overline{c}_R \sigma^{\mu\nu} b_L)(\overline{\tau}_R \sigma_{\mu\nu} \nu_L)\,.$$

$B \to D^{(*)}$ Form Factors in HQET

$$
\begin{aligned}
\langle D(k)|\bar{c}\gamma^\mu b|\overline{B}(p)\rangle &= \sqrt{m_B m_D}\left[h_+(w)(v+v')^\mu + h_-(w)(v-v')^\mu\right] \\
\langle D(k)|\bar{c}b|\bar{B}(p)\rangle &= \sqrt{m_B m_D}(w+1)h_S(w)\,, \\
\langle D(k)|\bar{c}\sigma^{\mu\nu}b|\bar{B}(p)\rangle &= -i\sqrt{m_B m_D}h_T(w)(v^\mu v'^\nu - v^\nu v'^\mu)\,, \\
\langle D^*(k,\epsilon)|\bar{c}\gamma^\mu b|\bar{B}(p)\rangle &= i\sqrt{m_B m_{D^*}}\,h_V(w)\varepsilon^{\mu\nu\rho\sigma}\epsilon^*_\nu v'_\rho v_\sigma\,, \\
\langle D^*(k,\epsilon)|\bar{c}\gamma^\mu\gamma^5 b|\bar{B}(p)\rangle &= \sqrt{m_B m_{D^*}}\left[h_{A_1}(w)(w+1)\epsilon^{*\mu}\right. \\
&\quad \left.-(\epsilon^*\cdot v)\left(h_{A_2}(w)v^\mu + h_{A_3}(w)v'^\mu\right)\right], \\
\langle D^*(k,\epsilon)|\bar{c}\gamma^5 b|\bar{B}(p)\rangle &= -\sqrt{m_B m_{D^*}}\,(\epsilon^*\cdot v)h_P(w), \\
\langle D^*(k,\epsilon)|\bar{c}\sigma^{\mu\nu}b|\bar{B}(p)\rangle &= -\sqrt{m_B m_{D^*}}\,\varepsilon^{\mu\nu\rho\sigma}\Big[h_{T_1}(w)\epsilon^*_\rho(v+v')_\sigma + h_{T_2}(w) \\
&\quad +h_{T_3}(w)(\epsilon^*\cdot v)v_\rho v'_\sigma\Big]\,,
\end{aligned}
$$

where the dimensionless kinematic variable $w = v\cdot v' = \frac{m_B^2+m_D^2-q^2}{2m_B m_D}$ is used instead of the momentum transfer $q^2 = (p-k)^2$.

In the heavy quark limit, only the single leading Isgur-Wise function $\xi(w)$ is needed for expressing the $B \to D^{(*)}$ form factors. With inclusion of the $\mathcal{O}(\alpha_s, \Lambda_{\rm QCD}/m_{b,c})$ contributions, these form factors are written as

$$
\begin{aligned}
h_+ &= \xi\left\{1 + \hat{\alpha}_s\left[C_{V_1} + \frac{w+1}{2}\left(C_{V_2} + C_{V_3}\right)\right] + \left(\varepsilon_c + \varepsilon_b\right)\hat{L}_1\right\}, \\
h_- &= \xi\left[\hat{\alpha}_s\,\frac{w+1}{2}\left(C_{V_2} - C_{V_3}\right) + \left(\varepsilon_c - \varepsilon_b\right)\hat{L}_4\right], \\
h_S &= \xi\left[1 + \hat{\alpha}_s\, C_S + \left(\varepsilon_c + \varepsilon_b\right)\left(\hat{L}_1 - \hat{L}_4\,\frac{w-1}{w+1}\right)\right], \\
h_T &= \xi\left[1 + \hat{\alpha}_s\left(C_{T_1} - C_{T_2} + C_{T_3}\right) + \left(\varepsilon_c + \varepsilon_b\right)\left(\hat{L}_1 - \hat{L}_4\right)\right], \\
&\ldots
\end{aligned}
$$

F. U. Bernlochner, Z. Ligeti, M. Papucci and D. J. Robinson, Phys. Rev. D **95**, *no. 11, 115008 (2017)*

The $L_{1\ldots6}$ functions can be expressed in terms of the sub-leading Isgur-Wise functions through:

$$\hat{L}_1 = -4(w-1)\hat{\chi}_2 + 12\hat{\chi}_3\,, \qquad \hat{L}_2 = -4\hat{\chi}_3\,, \qquad \hat{L}_3 = 4\hat{\chi}_2\,,$$
$$\hat{L}_4 = 2\eta - 1\,, \qquad \hat{L}_5 = -1\,, \qquad \hat{L}_6 = -2(1+\eta)/(w+1)\,.$$

With $\hat{\chi}_3(1) = 0$ implied by the Luke's theorem, up to $\mathcal{O}(\varepsilon_{c,b}(w-1))$ the subleading Isgur-Wise functions can be approximated as follows:

$$\hat{\chi}_2(w) \simeq \hat{\chi}_2(1) + \hat{\chi}_2'(1)(w-1)\,, \quad \hat{\chi}_3(w) \simeq \hat{\chi}_3'(1)(w-1)\,,$$
$$\eta(w) \simeq \eta(1) + \eta'(1)(w-1)\,.$$

Global Fit of the HQET Parameters

M. Jung and D. M. Straub, JHEP **1901**, *009 (2019)*

- Lattice QCD at zero hadronic recoil
- Light-cone sum rule at large hadronic recoil
- Strong unitarity constraints
- 1S Scheme (ensuring the renormalon cancellation)

$$\begin{pmatrix} \chi_2(1) \\ \chi_2'(1) \\ \chi_3'(1) \\ \eta(1) \\ \eta'(1) \\ \rho^2 \\ c \\ \delta_{h_{A_1}} \\ \delta_{h_+} \end{pmatrix} = \begin{pmatrix} -0.058 \pm 0.019 \\ -0.001 \pm 0.020 \\ 0.035 \pm 0.019 \\ 0.358 \pm 0.043 \\ 0.044 \pm 0.125 \\ 1.306 \pm 0.059 \\ 1.220 \pm 0.109 \\ -2.299 \pm 0.394 \\ 0.485 \pm 0.269 \end{pmatrix},$$

$$
\begin{pmatrix}
1.00 & 0.01 & 0.02 & -0.00 & 0.02 & -0.27 & -0.21 & -0.03 & 0.02 \\
0.01 & 1.00 & -0.00 & -0.02 & -0.02 & 0.00 & 0.14 & 0.01 & 0.00 \\
0.02 & -0.00 & 1.00 & 0.00 & -0.03 & 0.83 & 0.61 & -0.03 & 0.02 \\
-0.00 & -0.02 & 0.00 & 1.00 & 0.03 & 0.01 & 0.04 & 0.15 & 0.21 \\
0.02 & -0.02 & -0.03 & 0.03 & 1.00 & -0.14 & -0.16 & -0.05 & -0.22 \\
-0.27 & 0.00 & 0.83 & 0.01 & -0.14 & 1.00 & 0.79 & 0.09 & -0.14 \\
-0.21 & 0.14 & 0.61 & 0.04 & -0.16 & 0.79 & 1.00 & 0.06 & -0.08 \\
-0.03 & 0.01 & -0.03 & 0.15 & -0.05 & 0.09 & 0.06 & 1.00 & -0.24 \\
0.02 & 0.00 & 0.02 & 0.21 & -0.22 & -0.14 & -0.08 & -0.24 & 1.00
\end{pmatrix}
$$

$B_c \to J/\psi(\eta_c)$ Form Factors

$$\langle \eta_c(k)|\bar{c}\gamma_\mu b|B_c(p)\rangle = \left[(p+k)_\mu - \frac{m^2_{B_c} - m^2_{\eta_c}}{q^2} q_\mu\right] F_1(q^2) + q_\mu \frac{m^2_{B_c} - m^2_{\eta_c}}{q^2} F_0(q^2)\,,$$

$$\langle J/\psi(k)|\bar{c}\gamma^\mu b|B_c(p)\rangle = -\frac{2iV(q^2)}{m_{B_c} + m_{J/\psi}} \varepsilon^{\mu\nu\rho\sigma} \epsilon^*_\nu p_\rho k_\sigma\,,$$

$$\begin{aligned}\langle J/\psi(k)|\bar{c}\gamma^\mu\gamma^5 b|B_c(p)\rangle = {} & 2m_{J/\psi} A_0(q^2) \frac{\epsilon^* \cdot q}{q^2} q^\mu + (m_{B_c} + m_{J/\psi}) A_1(q^2) \left[\epsilon^{*\mu} - \frac{\epsilon^* \cdot q}{q^2} q^\mu\right] \\ & - A_2(q^2) \frac{\epsilon^* \cdot q}{m_{B_c} + m_{J/\psi}} \left[p^\mu + k^\mu - \frac{m^2_{B_c} - m^2_{J/\psi}}{q^2} q^\mu\right]\,,\end{aligned}$$

where the form factors are parametrized as $F(q^2) = F(0)\,\exp(c_1\hat{s} + c_2\hat{s}^2)$ with $\hat{s} = q^2/m^2_{B_c}$ in the full kinematical range of q^2, of which the results computed in the covariant light-front quark model.

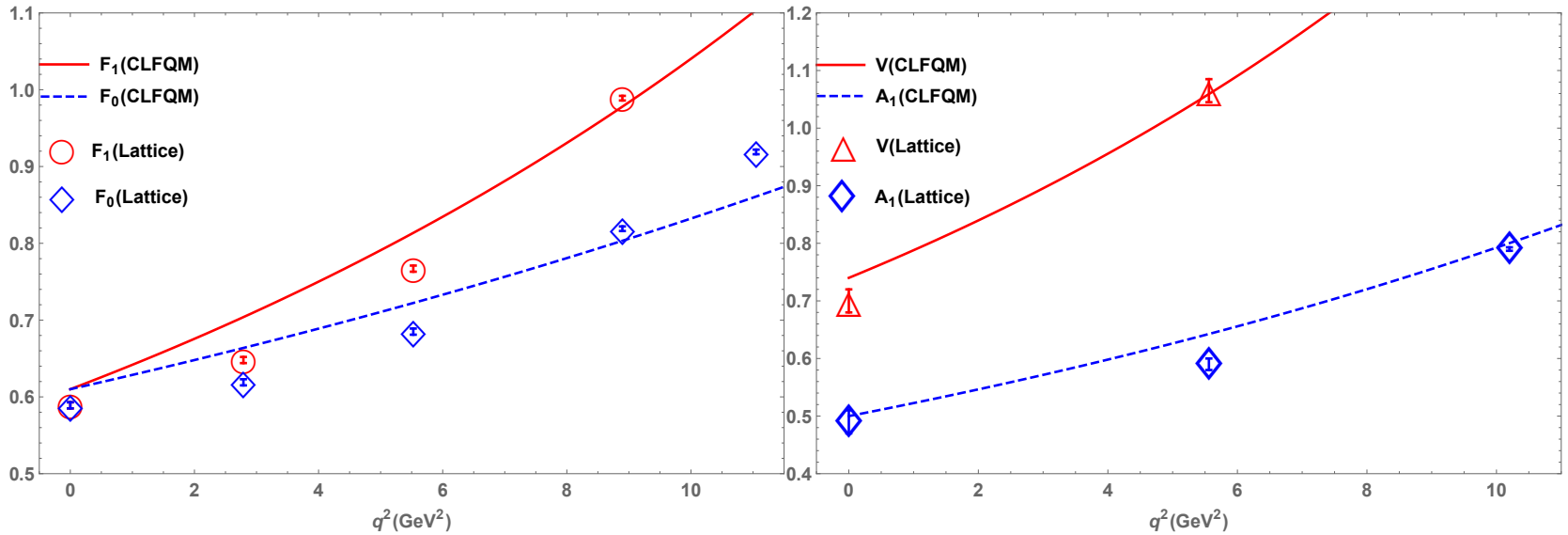

Figure: CLFQM form factors for the $B_c \to \eta_c$ and $B_c \to J/\psi$ hadronic transitions in comparison with the preliminary lattice results.

W. Wang, Y. L. Shen and C. D. Lu, Phys. Rev. D **79**, *054012 (2009)*
B. Colquhoun et al. [HPQCD Collaboration], PoS LATTICE **2016**, *281 (2016)*

χ^2 Fit of the Wilson Coefficients

χ^2 as a function of the Wilson coefficient C_X:

$$\chi^2(C_X) = \sum_{m,n=1}^{\text{data}} (O^{th}(C_X) - O^{exp})_m (V^{exp} + V^{th})^{-1}_{mn} (O^{th}(C_X) - O^{exp})_n + \frac{(R^{th}_{J/\psi}(C_X) - R^{exp}_{J/\psi})^2}{\sigma^2_{R_{J/\psi}}},$$

Table: Experimental data used in the fit.

	R_D	R_{D^*}	Correlation	$P_\tau(D^*)$	$R_{J/\psi}$
BABAR, 12	0.440(58)(42)	0.332(24)(18)	−0.27	–	–
Belle, 15	0.375(64)(26)	0.293(38)(15)	−0.49	–	–
Belle, 16	–	0.302(30)(11)	–	–	–
Belle, 17	–	$0.270(35)(^{+0.028}_{-0.025})$	0.33	$-0.38(51)(^{+0.21}_{-0.16})$	–
LHCb, 15	–	0.336(27)(30)	–	–	–
LHCb, 18	–	0.291(19)(26)(13)	–	–	–
LHCb, 18	–	–	–	–	0.71(17)(18)

Table: Fitted values of the Wilson coefficients in different NP scenarios.

NP scenario	value	χ^2/dof	Correlation
C_{V_1}	$(1+Re[C_{V_1}])^2+(Im[C_{V_1}])^2=1.27(6)$	7.42/8	–
C_{V_2}	$0.057(50)\pm 0.573(73)i$	6.19/8	0.750
C_{S_1}	$0.405(91)$	15.5/8	–
C_{S_2}	$-1.05(30)\pm 1.09(12)i$	5.98/8	0.589
C_T	$0.24(11)\pm 0.13(8)i$	8.39/8	-0.993

1σ Constraints on the NP Scenarios

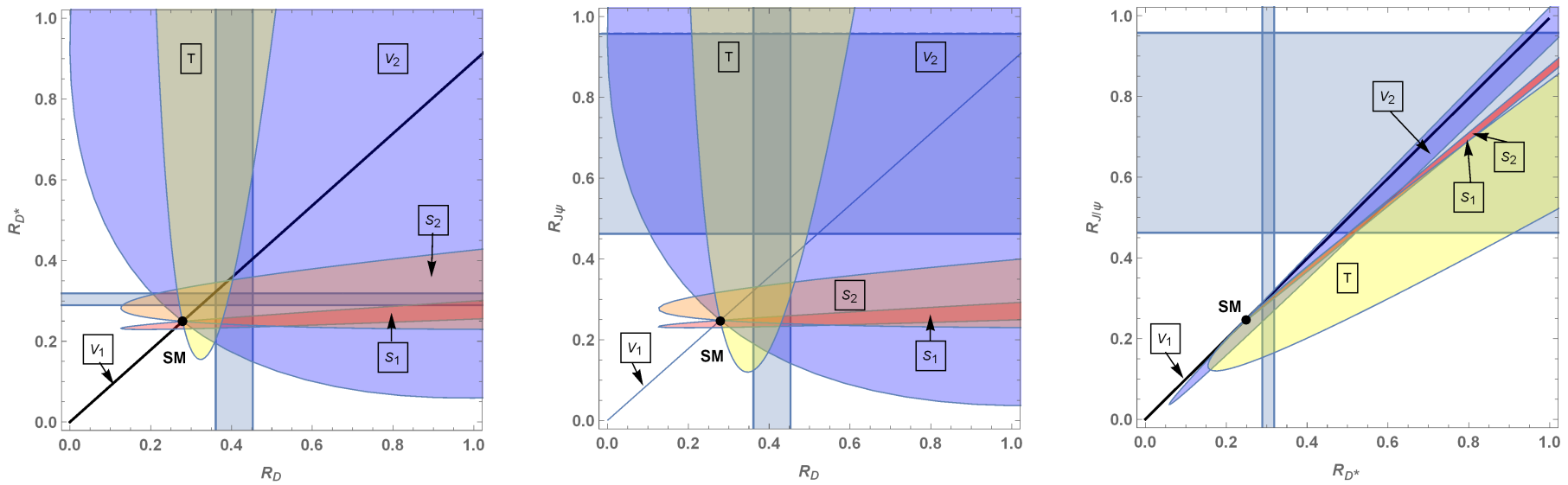

Figure: Correlations between $R(D)$, $R(D^*)$ and $R(J/\psi)$ in the presence of single NP operators. The vertical and horizontal bands show the experimental constraints and the black dots denote the SM predictions.

2σ Constraints on the NP Wilson coefficients

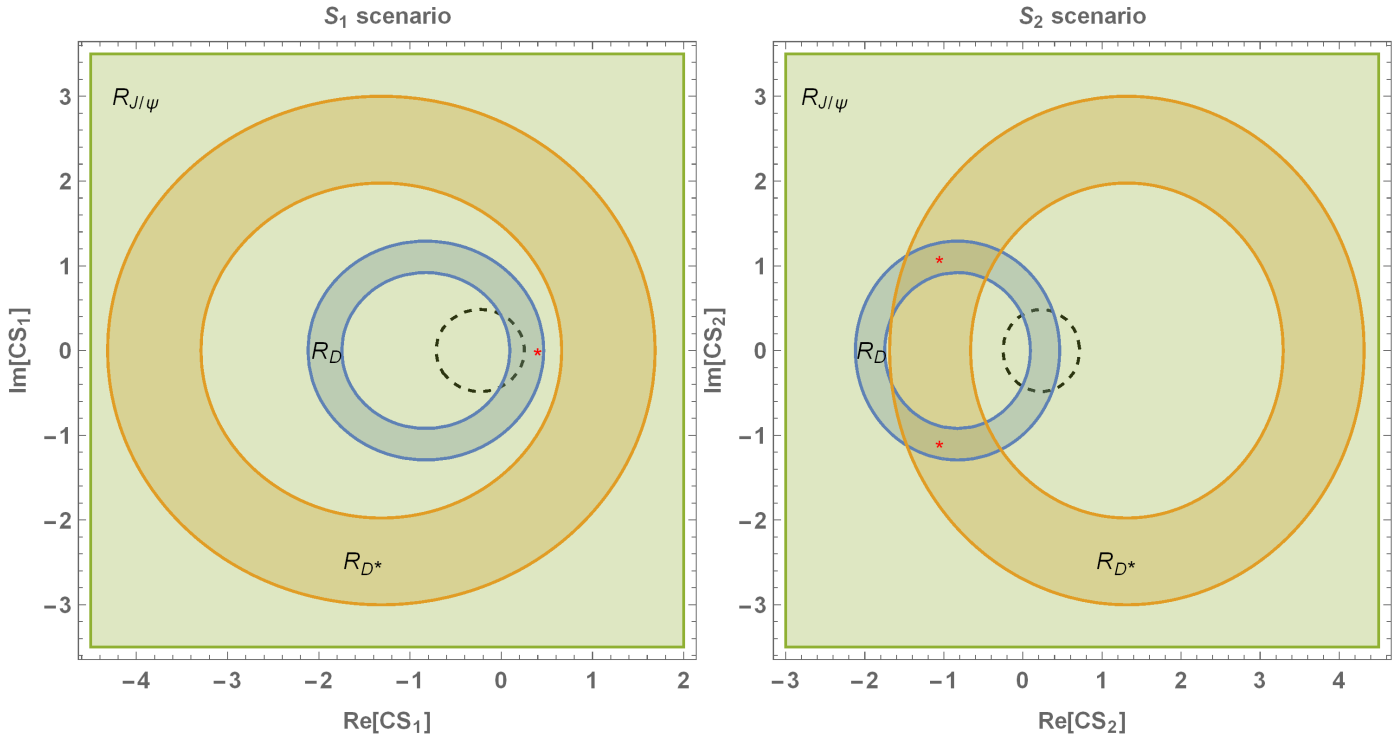

Figure: Constraints on the Wilson coefficients from the measurements of $R(D^{(*)})$ and $R(J/\psi)$ at the C.L. of 2σ and the branching fraction $\mathcal{B}(B_c \to \tau\nu)$ (black dashed curves). In each panel the red stars or dashed curves denote the optimal values obtained by using the fitted Wilson coefficients.

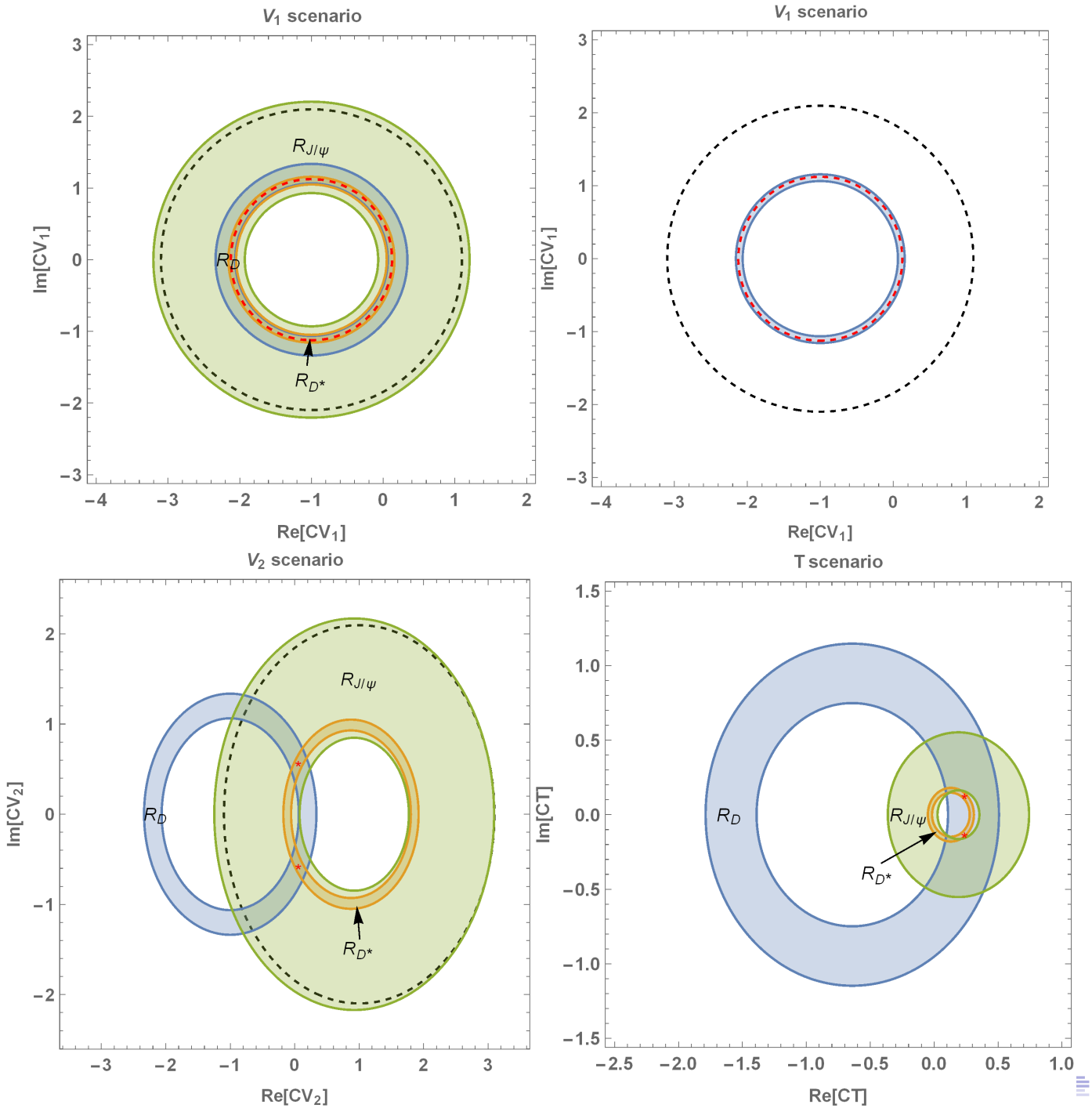
V_1 scenario
$R_{J/\psi}$
R_D
R_{D^*}
Im[CV_1]
Re[CV_1]
V_1 scenario
Im[CV_1]
Re[CV_1]
V_2 scenario
$R_{J/\psi}$
R_D
R_{D^*}
Im[CV_2]
Re[CV_2]
T scenario
R_D
$R_{J/\psi}$
R_{D^*}
Im[CT]
Re[CT]

Predictions for the Observables

Table: Predictions for observables involved in the $B \to D^{(*)}$ decays. The first and second uncertainties respectively result from the input parameters and the fitted Wilson coefficients.

Scenario	$R(D)$	$R(D^*)$	$P_\tau(D)$	$P_\tau(D^*)$	P_{D^*}	$\mathcal{A}_{FB}(D)$
SM	0.279(7)(0)	0.249(4)(0)	0.325(3)(0)	−0.508(4)(0)	0.441(6)(0)	0.3606(6)(0)
V_1	0.354(9)(19)	0.317(5)(17)	0.325(3)(0)	−0.508(4)(0)	0.441(6)(0)	0.3606(6)(0)
V_2	0.403(10)(48)	0.307(5)(15)	0.325(3)(0)	−0.509(4)(1)	0.436(7)(4)	0.3606(6)(0)
T	0.371(10)(42)	0.313(26)(15)	0.180(5)(49)	0.038(1)(118)	0.173(11)(60)	0.4311(5)(29)

Table: Predicted ranges for observables involved in the $B \to D^{(*)}$ decays from the experimental constraints within 2σ and the limit of $\mathcal{B}(B_c \to \tau\nu)$.

Senario	$R(D)$	$R(D^*)$	$P_\tau(D)$	$P_\tau(D^*)$	P_{D^*}	$\mathcal{A}_{FB}(D)$
V_1	[0.315, 0.373]	[0.282, 0.334]	[0.325, 0.325]	[−0.508, −0.508]	[0.441, 0.441]	[0.361, 0.361]
V_2	[0.315, 0.499]	[0.274, 0.334]	[0.325, 0.325]	[−0.511, −0.508]	[0.429, 0.441]	[0.361, 0.361]
T	[0.321,0.323]	[0.274, 0.334]	[0.248, 0.249]	[−0.234, −0.182]	[0.287, 0.306]	[0.395, 0.398]

Table: Predictions for observables involved in the $B_c \to \eta_c(J/\psi)$ decays. The first, second and third uncertainties respectively result from the input parameters, the fitted Wilson coefficients and the quark mass schemes for the tensor form factors.

Scenario	$R(\eta_c)$	$R(J/\psi)$	$P_\tau(J/\psi)$
SM	$0.281(^{+0.034}_{-0.030})(0)$	$0.248(6)(0)$	$-0.512(^{+0.021}_{-0.016})(0)$
V_1	$0.357(^{+0.044}_{-0.038})(19)$	$0.315(7)(17)$	$-0.512(^{+0.021}_{-0.016})(0)$
V_2	$0.406(^{+0.050}_{-0.044})(49)$	$0.304(7)(16)$	$-0.512(^{+0.021}_{-0.016})(1)$
T	$0.337(^{+0.019}_{-0.015})(26)(15)$	$0.188(^{+0.017}_{-0.012})(10)(21)$	$-0.028(^{+0.016}_{-0.013})(175)(53)$

$P_\tau(\eta_c)$	$P_{J/\psi}$	$\mathcal{A}_{FB}(\eta_c)$	$\mathcal{A}_{FB}(J/\psi)$
$0.347(81)(0)$	$0.446(6)(0)$	$0.364(^{+0.007}_{-0.009})(0)$	$-0.042(11)(0)$
$0.347(81)(0)$	$0.446(6)(0)$	$0.364(^{+0.007}_{-0.009})(0)$	$-0.042(11)(0)$
$0.347(81)(0)$	$0.443(6)(3)$	$0.364(^{+0.007}_{-0.009})(0)$	$0.031(7)(13)$
$0.24(^{+0.15}_{-0.13})(4)(2)$	$0.271(14)(64)(41)$	$0.419(^{+0.014}_{-0.031})(23)(8)$	$-0.036(^{+0.010}_{-0.008})(49)(21)$

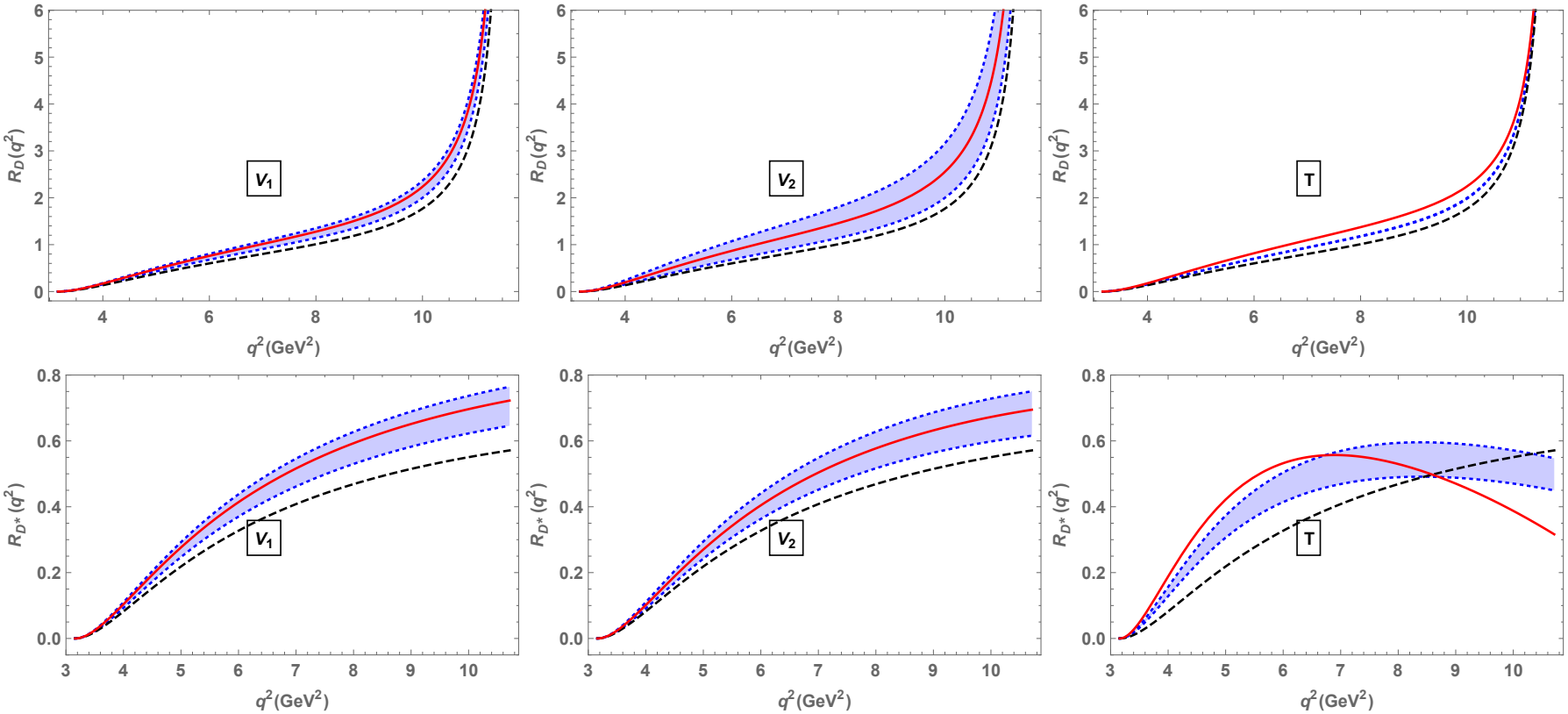

Figure: Predictions for the differential ratios $R_D(q^2)$ and $R_{D*}(q^2)$. The black dashed lines and the red solid lines respectively denote the SM predictions and the NP predictions corresponding to the best fitted Wilson coefficients. The light blue bands include NP effects corresponding to the experimental constraints within 2σ.

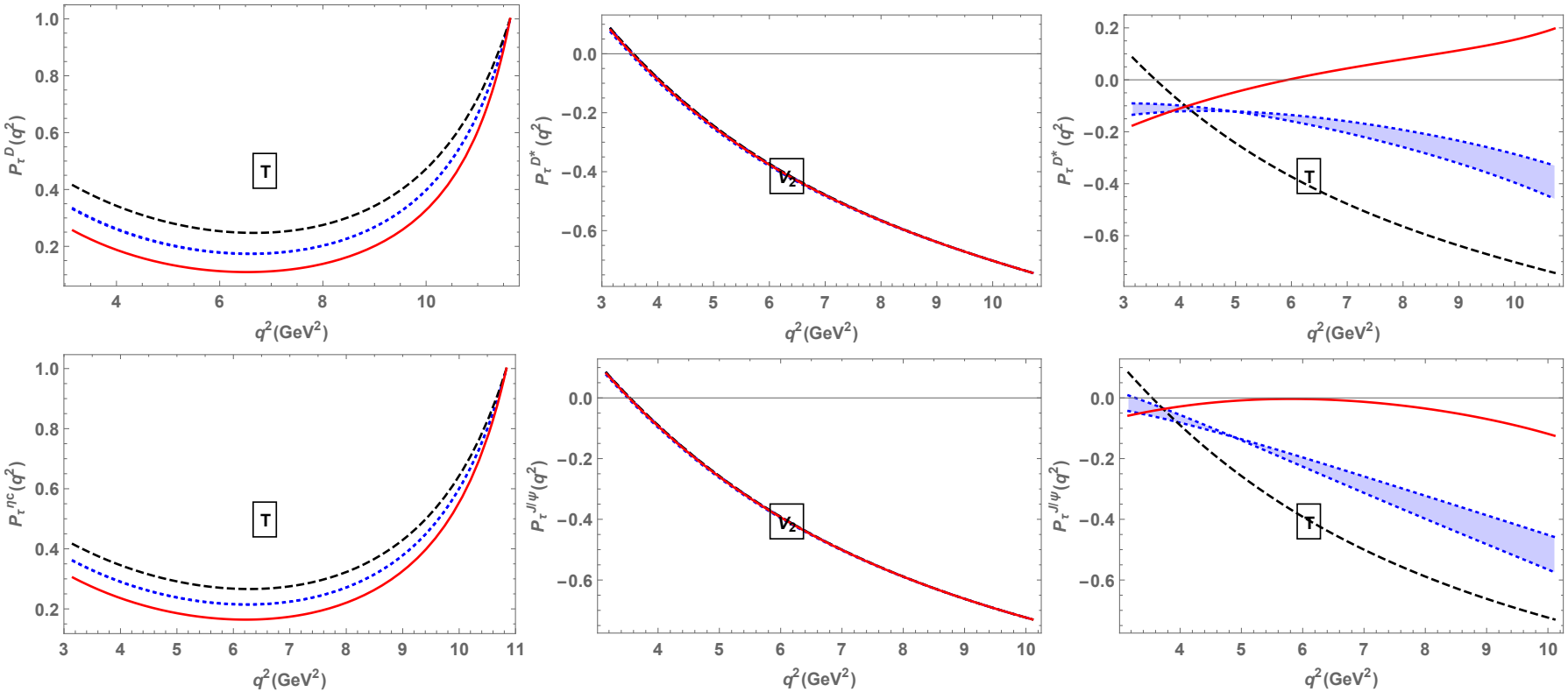

Figure: Predictions for the differential polarizations $P_\tau^{D^{(*)}}(q^2)$, $P_\tau^{\eta_c}(q^2)$ and $P_\tau^{J/\psi}(q^2)$. The black dashed lines and the red solid lines respectively denote the SM predictions and the NP predictions corresponding to the best fitted Wilson coefficients. The light blue bands include NP effects corresponding to the experimental constraints within 2σ.

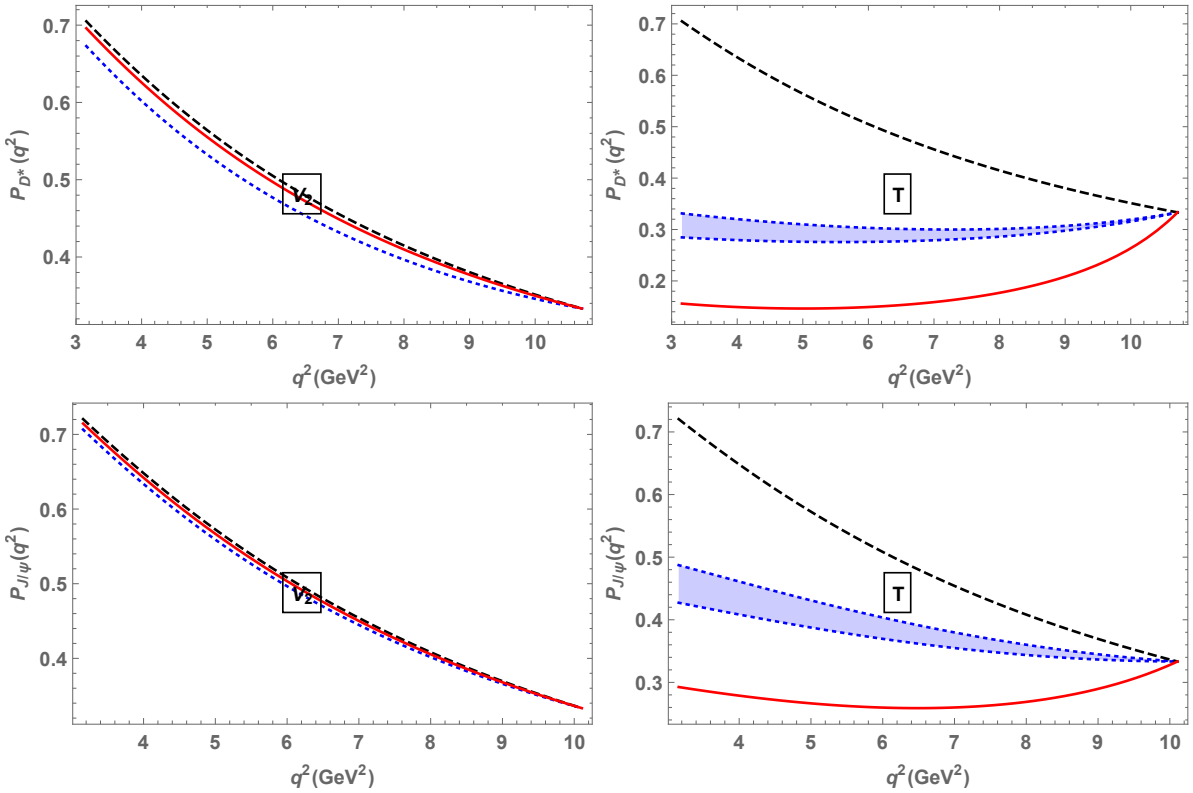

Figure: Predictions for the differential polarizations $P^{D^*}(q^2)$ and $P^{J/\psi}(q^2)$. The black dashed lines and the red solid lines respectively denote the SM predictions and the NP predictions corresponding to the best fitted Wilson coefficients. The light blue bands include NP effects corresponding to the experimental constraints within 2σ.

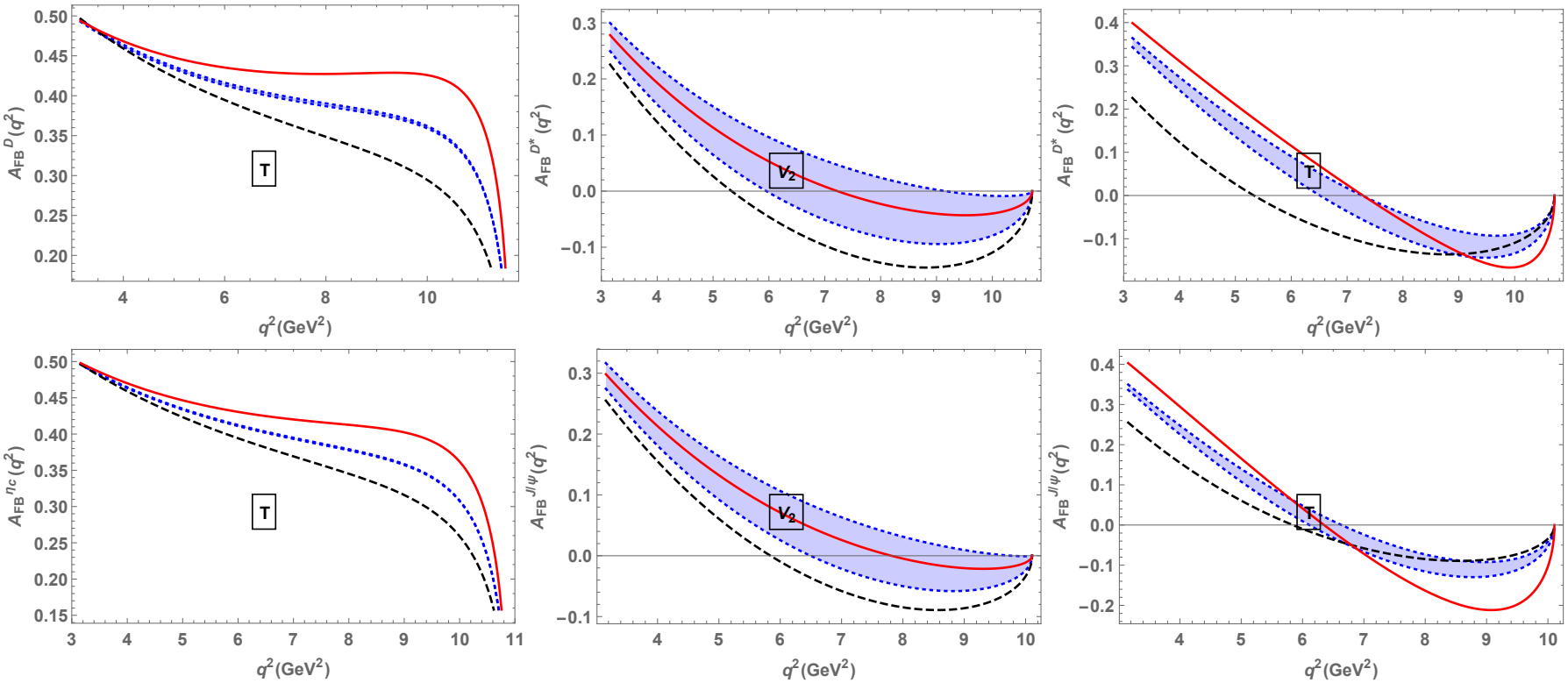

Figure: Predictions for the differential forward-backward asymmetries. The black dashed lines and the red solid lines respectively denote the SM predictions and the NP predictions corresponding to the best fitted Wilson coefficients. The light blue bands include NP effects corresponding to the experimental constraints within 2σ.

Summary and Conclusions

In the model-independent analysis of the new physics effects in the $b \to c\tau\nu$ transitions using the improved HQET form factors and CLFQM form factors, we find

- None of the single operators can explain simultaneously the current experimental measurements of $R(D)$, $R(D^*)$ and $R(J/\psi)$ within 1σ.
- Allowed regions for the Wilson coefficients of the vector and tensor operators (severely constrained) are obtained from the experimental constraints within 2σ along with the limit on $\mathcal{B}(B_c \to \tau\nu)$.
- In the minimum χ^2 fit to the experimental measurements of $R(D^{(*)})$, $R(J/\psi)$ and $P_\tau(D^*)$, the V_2 scenario gives the smallest χ^2 value among the allowed scenarios.

- Any NP model dominated by a single scalar or tensor operator is under challenge, such as some types of charged Higgs models.
- The $R(D^*)$ anomalies have been amplified given our SM predictions, while the predicted $R(D)$ and $R(D^*)$ in the V_2 scenario are in excellent agreement with the current world average values.
- We have made predictions for various physical observables relevant to the $B \to D^{(*)}\tau\nu$ and $B_c \to \eta_c(J/\psi)\tau\nu$ decays, namely R, P_τ, P_M, and $\mathcal{A}_{FB}$, and the corresponding q^2 distributions.

- Any NP model dominated by a single scalar or tensor operator is under challenge, such as some types of charged Higgs models.
- The $R(D^*)$ anomalies have been amplified given our SM predictions, while the predicted $R(D)$ and $R(D^*)$ in the V_2 scenario are in excellent agreement with the current world average values.
- We have made predictions for various physical observables relevant to the $B \to D^{(*)}\tau\nu$ and $B_c \to \eta_c(J/\psi)\tau\nu$ decays, namely R, P_τ, P_M, and $\mathcal{A}_{FB}$, and the corresponding q^2 distributions.

Thanks for your attention!